第 31 卷 第 4 期
2009 年 12 月

地球科学与环境学报
Journal of Earth Sciences and Environment

Vol. 31 No. 4
Dec. 2009

现今绝对板块运动

魏 子 卿
(西安测绘研究所, 陕西 西安 710054)

摘要: 根据热点假设, 热点对于中间层是固定的。相对热点的板块运动叫做绝对板块运动。绝对板块运动模型可以通过反演火山链传播的速率和走向数据以确定相对板块运动在角速度空间的原点来得到。利用一组近来(0~7.8 Ma)全球分布的热点的迁移速率和走向数据, 结合板块运动模型 NNR-NUVEL1A, 已研制出一个叫做 APM2 的现今绝对板块运动模型。按照该模型, 太平洋板块围绕 60.063°S、102.210°E 处的极以(0.833 0°±0.013 3°)/Ma 的速率运动, 非洲板块围绕 46.849°N、44.372°W 的极以(0.101 5°±0.013 4°)/Ma 的速率运动, 南极板块的运动则以 46.871°N、146.942°E 为极, 速率为(0.084 6°±0.017 7°)/Ma, 欧亚板块的运动更慢, 极为 27.291°N、171.925°W, 速率为(0.065 5°±0.020 6°)/Ma。这一模型表明, 岩石圈相对深部地幔有一个以 49.423°S、90.625°E 为极, 速率为(0.198 3°±0.013 5°)/Ma 的净旋转。表明太平洋热点同印度—大西洋热点不一致, 显示太平洋热点的运动也不一致。为了分析和比较, 还给出了仅用全球分布的热点的走向数据和仅用印度—大西洋热点的走向数据得到的板块绝对运动的角速度。

关键词: 绝对板块运动; 热点; 热点参考架; 无净旋转参考架; 岩石圈的净旋转
中图分类号: P227 文献标志码: A 文章编号: 1672-6561(2009)04-0331-13

Current Absolute Plate Motions

WEI Zi-qing
(*Xi'an Research Institute of Surveying and Mapping, Xi'an* 710054, *Shaanxi, China*)

Abstract: The plate motions with respect to the hotspots, which are fixed relative to the mesosphere according to the hotspot hypothesis, are called absolute. The absolute plate motion model can be achieved by inverting the data set of the propagation rates and/or trends of volcanic chains to determine the origin in the angular space for the relative plate motion. A current absolute plate motion model designated as APM2 has been developed using a data set of migration rates and trends of recent (0~7.8 Ma) globally distributed hotspots tracks in conjunction with the plate motion model NNR-NUVEL1A. According to this model, the Pacific plate is moving at a rate of (0.833 0°±0.013 3°)/Ma about a pole at 60.063°S, 102.210°E; Africa has a motion of (0.101 5°±0.013 4°)/Ma about 46.849°N, 44.372°W; Antarctic has a motion of (0.084 6°±0.017 7°)/Ma about 46.871°N, 146.942°E; Eurasia has an even slower motion of (0.0655°±0.0206°)/Ma about 27.291°N, 171.925°W. The model shows that the lithosphere has a net rotation of (0.198 3°±0.013 5°)/Ma about 49.423°S, 90.625°E with respect to the deep mantle. It is demonstrated that the Pacific hotspots are inconsistent with the Indo-Atlantic hotspots. Also, it is shown that the Pacific hotspots involved appear do not have a coherent motion. For analysis and comparison, this paper also gives the angular velocities of absolute plate motions obtained from only trend data for global distributed hotspots and from only trend data for only Indo-Atlantic hotspots.

Key words: absolute plate motion; hotspots; hotspot reference frame; no-net-rotation reference frame; net rotation of the lithosphere

0 Introduction

A number of absolute plate motion models[1-5] have been developed based on the hotspot hypothesis[6-7], by inverting the data set of the propagation rates and/or trends of volcanic chains to de-

收稿日期: 2009-07-28
作者简介: 魏子卿(1937-), 男, 河南睢县人, 研究员, 从事大地测量与地球动力学研究。E-mail: ziqingw@public.xa.sn.cn

termine an origin in the angular velocity space for the relative plate motion. In terms of the way the hotspot data are utilized, absolute plate models may be grouped into two categories: the first category, to which the model AM1[5] belongs, use only trend data; the second category, including AM1-2[2], HS2-NUVEL1[4] and HS3-NUVEL1A[5], employ both trends and rates, generally just spanning a single hemisphere (e.g. the Pacific hemisphere). The AM1-2 and HS2-NUVEL1 share the same dataset consisting of 5 rates and 9 trends over the Pacific, Cocos and Nazca and North America; the HS3-NUVEL1A uses a recalculated set of data composed of 2 rates and 11 trends, which again only span the Pacific hemisphere. Müller et al developed the revised plate motions relative to the hotspots by combining the hotspot tracks in the Atlantic and Indian Oceans without using those in the Pacific Ocean[8].

We have found that the speed as well as the direction of plate motion for the same plate may differ significantly from one model to another. For example, for Eurasia some models show a clockwise rotation, while others anti-clockwise; the similar situation occurs for Africa and other plates. This puzzling problem is likely to be related to the geometry of hotspot tracks used by individual authors. It is conceivable that if the hotspots were fixed with respect to one another and if the relative motion model was right the hotspots situated on one single plate would be adequate for determining the absolute plate motion. However, the hotspots are in fact not fixed with respect to each other, and furthermore, the hotspot tracks on the Pacific plate are not consistent with those on the Indo-Atlantic Oceans[9], so the absolute motion model is strongly hotspot dependent. It would be desirable for achieving a better absolute plate motion model to use a set of well-distributed hotspot tracks, both in the Indo-Atlantic hemisphere and in the Pacific hemisphere, but, as shown later on, the global reference frame is essentially defined by the Indo-Atlantic hotspots.

The rates and trends of hotspot migration are translated to the absolute plate motion in a different manner. The rates are more sensitive to the speed, while the trends are more sensitive to the direction of plate motion, but less to the episodicity and nonlinearity of the motion, which may occur for some plates[10-12]. Naturally, it would be better to use the rates and trends together rather than either kind of data alone; this is the way we are trying to do. In an attempt to solve the puzzle mentioned above an absolute plate motion model is developed in this paper by using the rate and trend data associated with both the Pacific and the Indo-Atlantic hotspots. We address the reference frames in Section 1, describe the data and methodology in Sections 2 and 3, and present the results and give discussions in Sections 4 and 5. The paper is concluded in Section 6.

1 Reference Frames

Traditionally the hotspot reference frame has been used to measure the absolute motion of the plates[13], which is based on the assumption that the hotspots are fixed relative to the mesosphere and that the trends and the age progressions of the linear island reflect the motion of the overlying lithospheric plate relative to the hotspots. The fixity of the hotspots has been tested by numerous investigators (e.g. [14-17] among others). Studies show that the hotspots in the Atlantic and Indian Oceans have no significant motion (less than 5 mm/a) between these plumes[8,15-17], thus can served as a coherent Indo-Atlantic hotspot reference frame. However, studies also show the Hawaiian hotspot has migrated south at a rate of over 40mm/a for the period from 81 to 47 Ma ago[18]. Moreover, it has long been aware that there is a large misfit between observed and hypothetical Pacific hotspot tracks predicted in a reference frame fixed to Atlantic and Indian Ocean hotspots, and vice versa[9]. As Divenere et al[19] demonstrated, the often-cited East-West Antarctic motions cannot account for the apparent motion between the

Hawaiian-Emperor hotspot and the Indo-Atlantic hotspots, and it is concluded that the inter-hemispheric relative motion between the Indo-Atlantic hotspots and Pacific hotspots (at least the Hawaiian-Emperor hotspot) appears likely. If this is the case, the hotspots will not define a fixed reference frame on the global scale. Nevertheless, today's state-of-arts constrain us to choose the hotspot reference frame to measure the absolute motion of the plates even though it is merely a quasi-fixed reference frame. We believe the non-fixity of the hotspots will not jeopardize the conclusions to be drawn. So in this study we still use the hotspot frame as a basic frame, and try to use the Pacific as well as the Indo-Atlantic hotspots to define the hotspot reference frame.

As pointed out earlier that the key point of deriving the absolute plate motion model is to invert the hotspot track data to determine the origin in the angular velocity space for the relative plate motion. The relative plate motion model is usually constructed in the no-net-rotation frame (Also known as the mean-lithosphere frame) defined such that it yields a zero for the integral of $\boldsymbol{v}\times\boldsymbol{r}$ over the Earth's surface, where $\boldsymbol{v}$ is the plate velocity at position $\boldsymbol{r}$; sign $\times$ denotes vector cross product(cf. [20]). It is worthwhile to note that the no-net-rotation frame itself is not fixed relative to the mesosphere, instead drift along with the lithosphere.

Let ω_h be the angular velocity vector of a plate in the hotspot frame, ω_n the angular velocity vector of the plate in the no-net rotation frame, and ω_{nr} the net rotation velocity vector of the lithosphere in the hotspot frame, we can write out the relation among the three vectors

$$\omega_h = \omega_n + \omega_{nr} \tag{1}$$

On the basis of equation (1), we can readily obtain the following relations between the rotation vectors (pole φ, λ and angular velocity ω) of a plate in the two frames

$$\omega_h = \{\omega_n^2+\omega_{nr}^2+2\omega_n\omega_{nr}[\sin\varphi_n\sin\varphi_{nr}+\cos\varphi_n\cos\varphi_{nr}\cos(\lambda_n-\lambda_{nr})]\}^{\frac{1}{2}} \tag{2}$$

$$\sin\varphi_h=\frac{\omega_n}{\omega_h}\sin\varphi_n+\frac{\omega_{nr}}{\omega_h}\sin\varphi_{nr} \tag{3}$$

$$\tan\lambda_h=\frac{\omega_n\cos\varphi_n\sin\lambda_n+\omega_{nr}\cos\varphi_{nr}\sin\lambda_{nr}}{\omega_n\cos\varphi_n\cos\lambda_n+\omega_{nr}\cos\varphi_{nr}\cos\lambda_{nr}} \tag{4}$$

where ω_h, ω_n and ω_{nr} are respectively the magnitude of angular velocity of a plate in the hotspot and in the no-net-rotation frame and of the net rotation of the lithosphere; λ_n, φ_n are the longitude and latitude of the rotation pole of a plate in the no-net rotation frame; λ_{nr}, φ_{nr} are the longitude and latitude of the pole of the net rotation of lithosphere in the hotspot frame.

2 Data

To derive the current absolute plate motion model, we use the young hotspot data in conjunction with the relative plate model NUVEL1-A, which averages plate motion over a time span less than ≈3.2 Ma[21]. We confine ourselves to use the hotspot data spanning for a ≈7.8 Ma time interval, so that by the current absolute plate motion we mean the plate motion spanning less than 7.8 Ma BP with respect to the hotspot reference frame. Considering many tectonic events took place from 4 Ma to 8 Ma, such as slowdown in spreading rate along southern mid-Atlantic Ridge in 8~4 Ma[22] and changes in African absolute motion at 6 Ma[23], it would be less meaningful to talk about the current plate motion when averaging the plate motion over more than for example 8 Ma.

The hotspot data we used are listed in table 1, including 8 rates and 20 trends involving 20 hotspot tracks, distributed on 7 plates over both the Pacific and the Atlantic hemispheres as shown in figure 1. Amongst these 2 rates and 11 trends are quoted from [5] in constructing the model HS3-NUVEL1A which averages the plate motion over the past ≈5.8 Ma, and the remaining data cited from other literatures. It should be pointed out that modifications have been made for some rates to accommodate them to a 7.8 Ma time interval. For example, for the Austral Island chain, we use the data in [24] and regress age, as dependent

Tab. 1 Observed and Modeled Values for Rates and Trends

Hotspot	Plate	Location		Observed	Modeled	Observed—Modeled	Geometric Contribution	Y_1	Y_2	Reference
		°N	°E	±1σ	±1σ					
				Rates/(mm·a^{-1})						
Hawaii	PAC	20.65	−156.91	108.0±5.0	85.3±1.5	22.7±5.2	6375.5	0.28	0.66	[5]
Society	PAC	−17.33	−149.95	106.0±9.0	92.1±1.5	13.9±9.1	6376.3	0.011	0.011	[5]
Foundation	PAC	−37.75	−110.80	77.3±8.4	90.8±1.5	−13.5±8.5	6370.2	0.013	0.013	This paper
Marquesas	PAC	−9.59	−139.37	101.3±17.5	92.3±1.4	9.0±17.6	6377.5	0.000 3	0.000 3	[25]
Austral Island	PAC	−29.00	−140.00	92.8±9.8	90.5±1.5	2.3±9.9	6373.1	0.000 2	0.000 2	This paper
St.Helena Island	AFR	−16.38	−9.01	11.6±1.4	10.7±1.4	0.9±2.0	6376.4	0.80	0.25	This paper
Tristan	AFR	−37.20	−12.30	16.0±5.0	11.3±1.5	4.7±5.2	6370.4	0.014	0.013	This paper
Vema	AFR	−32.00	8.50	16.0±5.0	11.3±1.5	4.7±5.2	6 372.2	0.014	0.013	This paper
				Trends/(°)						
Hawaii	PAC	20.65	−156.91	303.5±6.3	302.2±0.9	1.3±6.4	74.8	0.000 1	0.000 1	[5]
Society	PAC	−17.33	−149.95	292.6±7.8	298.6±1.1	−6.0±7.9	69.2	0.001 9	0.001 9	[5]
Foundation	PAC	−37.75	−110.80	297.0±10.0	286.1±1.4	10.9±10.1	70.2	0.003 9	0.003 8	This paper
Marquesas	PAC	−9.59	−139.37	310.0±12.3	296.1±1.2	13.9±12.4	69.1	0.001 9	0.001 8	[5]
Macdonald	PAC	−28.31	−142.31	291.0±8.7	297.5±1.3	−6.5±8.8	70.5	0.001 9	0.001 8	[5]
Pitcairn	PAC	−25.21	−129.59	289.1±35.9	293.2±1.3	−4.1±35.9	69.0	0.000 0	0.000 0	[5]
Samoa	PAC	−14.19	−170.74	283.2±11.2	300.9±0.9	−17.7±11.2	70.8	0.002 5	0.002 7	[5]
Easter	NAZ	−27.11	−110.06	98.6±31.7	94.4±2.2	4.2±31.8	108.9	0.000 0	0.000 0	[5]
Galapagos	NAZ	−0.54	−90.83	121.3±40.9	78.2±2.6	43.1±41.0	139.1	0.000 7	0.000 7	[5]
Juan Fernandez	NAZ	−33.73	−80.45	86.4±14.0	74.2±2.0	12.2±14.1	105.5	0.002 3	0.002 3	[5]
Martin Vaz	SAM	−20.49	−29.09	264.9±52.7	268.1±3.5	−3.2±52.8	268.1	0.000 0	0.000 0	[5]
Yellowstone	NAM	44.38	−111.05	241.0±23.8	256.0±6.6	−15.0±24.7	344.9	0.005 1	0.004 7	[5]
St.Helena	AFR	−16.38	−9.01	64.0±10.0	65.2±5.8	−1.2±11.6	597.9	0.001 6	0.001 2	This paper
Tristan	AFR	−37.20	−12.30	70.0±10.0	68.7±6.1	1.3±11.7	564.4	0.002 1	0.001 5	[23]
Vema	AFR	−32.00	8.50	60.0±10.0	56.9±5.4	3.1±11.4	564.6	0.008 0	0.006 1	[23]
Reunion	AFR	−21.20	55.70	45.0±10.0	43.4±9.3	1.6±13.7	608.4	0.018 0	0.007 0	[23]
Prince Edward	AFR	−43.10	37.50	38.0±15.0	41.6±6.4	−3.6±16.3	623.6	0.002 4	0.002 0	[23]
Discovery	AFR	−42.50	−2.00	65.0±15.0	62.3±5.8	2.7±16.1	568.2	0.001 1	0.000 9	[23]
Kerguelen	ANT	−49.00	69.00	140.0±15.0	138.7±11.4	1.3±18.8	761.0	0.002 1	0.001 1	[26]
Galapagos	COC	−1.00	−92.00	45.0±15.0	41.5±1.0	3.5±15.0	76.7	0.000 0	0.000 0	[1]

The Meanings of Y_1 and Y_2 are Shown in Equation 11

variable, on distance X from Macdonald to Raivavae, the following equation being obtained

$$Age(\text{Ma}) = (0.010\,770\,322 \pm 0.001\,134\,551)X + (0.000\,007\,512 \pm 0.005\,418\,091)$$

thereby achieving a rate of 92 8 mm/a, with a standard deviation of 9. 8 mm/a.

For the Tristan and Vema hotspots, we utilize the rates given by Pollitz[23], but subtracted by a southwesterly shift of 8 mm/a, which is the difference between the pre-6 Ma and post-6 Ma African absolute plate motions evaluated at 6 Ma by Pollitz[23].

For the Foundation chain, we regress age (≤7. 7 Ma) on the distance (700 km) between seamounts No. 30 and 22, using data in [27], obtaining

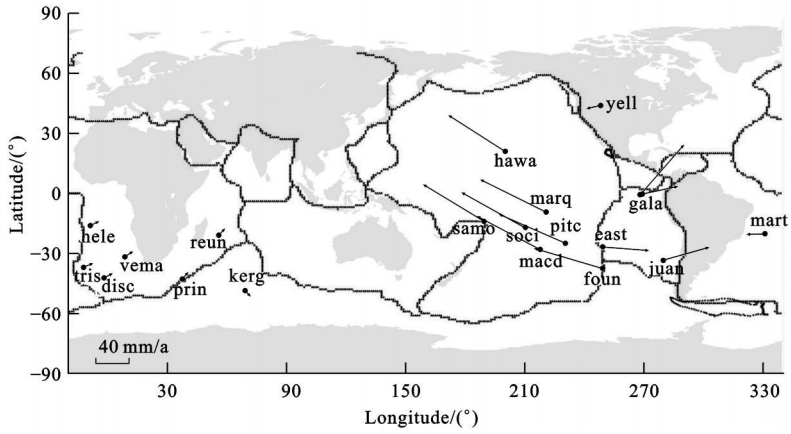

Fig. 1　Geographic Distribution of the Hotspots Used and Predicted Progression Rates of Volcanic Chains

$$Age(\mathrm{Ma}) = (0.012\,931\,419 \pm 0.001\,411\,060)X - (0.742\,874\,697 \pm 0.715\,839\,216)$$

thus giving a rate of 77.3 mm/a with a standard deviation of 8.4 mm/a.

For the St. Helena Island, we use the age data (≤7.8 Ma) of the seamounts Josephine and Benjamin in [28], obtaining a rate of 11.6 mm/a with a standard deviation of 1.4 mm/a.

In our inversion, each hotspot datum is assigned a standard error based on its uncertainty. For the data in [5], the uncertainties are objectively determined from the dispersion of volcano age and location; for other published data quoted here, the trends were obtained from bathymetric charts[1-2], among which some maybe involve the averaging interval greater than 7.8 Ma, and were subjectively assigned an uncertainty of 10° or 15°. As our results show later on, the uncertainties are in general good approximations to their standard errors, but probably most tend to be conservatively estimated.

In column 8 of table 1 listed is a quantity, "geometric contribution (GC)", defined as

$$GC = \sqrt{\left(\frac{\partial d}{\partial \omega_x}\right)^2 + \left(\frac{\partial d}{\partial \omega_y}\right)^2 + \left(\frac{\partial d}{\partial \omega_z}\right)^2} \qquad (5)$$

to measure the role played by a datum d in determining the plate motion model, where in radical sign is the sum of the partial derivatives squared of the datum with respect to the x-, y and z components of angular velocity ω. The units are in km for rate and in Ma for trend. The quantity is similar in concept to the "importance" used by others (e.g. [1, 29]).

In table 1 listed are the modeled values computed by our model and the "observed−modeled" values for each datum. All the 20 modeled trends but 4 (Foundation, Marquesas, Galapagos and Samoa) lie within their prescribed uncertainties; all the 8 modeled rates but 3 (Society, Foundation and Hawaii on the Pacific plate) lie within their respective uncertainties, while Hawaiian rate lies far beyond its uncertainty, attributed to either large dating error or most likely the relative motion between hotspots. Fortunately, they all pass the model robustness check, which will be described later on, as shown in table 1 (See items Y_1 and Y_2), so that there seems to be no point in rejecting them. On the contrary, the Hawaiian rate needs to be retained in the datum list to take into account the nonfixity and non-rigidity of the hotspot frame due in particular to the inconsistent motions between the Pacific and Atlantic hotspots.

3　Methodology

The observation data are inverted to estimate the angular velocities of plate motion relative to the hotspots by minimizing the following quantity using an iterative, weighted least square procedure[5, 29]

$$\chi^2 = \sum_{i=1}^{N}\left(\frac{d_i^{\mathrm{obs}} - d_i^{\mathrm{cal}}(\omega)}{\sigma_i}\right)^2 \qquad (6)$$

where d_i^{obs} is the ith datum (rate or trend); $d_i^{\mathrm{cal}}(\omega)$ is its value calculated from a priori motion model

ω, which consists of the rotation vectors describing the motion of each plate relative to the hotspots; σ_i is the standard error assigned to the ith datum and N is the total number of data. $d^{cal}(\omega)$ can be expressed by

$$v = \sqrt{v_n^2 + v_e^2} \quad \text{for rate} \tag{7}$$

$$A = \arctan \frac{v_e}{v_n} \quad \text{for trend} \tag{8}$$

with

$$v_n = r\sin\lambda\omega_x - r\cos\lambda\omega_y \tag{9}$$

$$v_e = -r\sin\varphi\cos\lambda\omega_x - r\sin\varphi\sin\lambda\omega_y + r\cos\varphi\omega_z \tag{10}$$

where v_n, v_e are the respective northing and easting components of linear velocity of a point of interest with spherical coordinates r(radius), φ(latitude) and λ(longitude); ω_x, ω_y, ω_z are the geocentric Cartesian x-, y- and z components of angular velocity respectively.

The model NNR-NUVEL1A[21] was used as the a priori plate motion model in the inversion. The model is a set of angular velocities, consistent with the relative plate motion model NUVEL-1A[21, 29], of the plates in a reference frame in which there is no net rotation of the lithosphere. In order to speed up the convergence of inversion, the NNR-NUVEL1A velocities are first approximately rotated into the hotspot reference frame by using the Pacific or (but not and) African plate rotation in a mean mantle reference frame given by [30] (This is preferable, but not mandatory). In other words, the inversion is practically initiated using the "absolute" Pacific (or African) velocity. The parameters solved for are three components of the correction vector for angular velocity vector of the Pacific (or African), or equivalently of any other plates. At this point it is important to note that the correction vector for the NNR-NUVEL1A velocities to be achieved is nothing else than the net rotation of the lithosphere (cf. Equation 1). We achieve the final solutions for angular velocities relative to hotspots by adding the correction vector thus obtained to the NNR-NUVEL1A velocities for each plate. It is found that the inversion is rather rapidly converged for which the criterion is specified such that the absolute value of increment correction for each of three components of angular velocity should be less than 0.000 01″/Ma.

We estimate uncertainties in angular velocity relative to hotspots by linear propagation of errors, neglecting small errors from the NUVEL1-A relative plate angular velocities. The error ellipses for rotation poles are obtained based on the covariance matrix of correction angular velocities.

To check the robustness of our model, we compare the correction vector for the NNR-NUVEL1A velocities from the whole data set with the alternative correction vector for the NNR-NUVEL1A derived by removing one datum and re-inverting the remaining data. Let $\Delta\omega$ denote the correction vector, $\Delta\omega'$ the alternative correction vector, $C_{\Delta\omega}^{-1}$ and $C_{\Delta\omega'}^{-1}$ the estimates of respective covariance matrices for $\Delta\omega$ and $\Delta\omega'$, the following statistics are defined

$$\begin{aligned} Y_1 &= \frac{1}{u}(\Delta\omega' - \Delta\omega)^{\mathrm{T}}\, C_{\Delta\omega'}^{-1}(\Delta\omega' - \Delta\omega) \\ Y_2 &= \frac{1}{u}(\Delta\omega - \Delta\omega')^{\mathrm{T}}\, C_{\Delta\omega}^{-1}(\Delta\omega - \Delta\omega') \end{aligned} \tag{11}$$

where Y_1 and Y_2 have a Fisher distribution $F_{u,m-u,\alpha}$ at a given significance level α with u degrees of freedom and m observations. In the comparison of $\Delta\omega'$ and $\Delta\omega$, if $Y_1 < F_{3,24,0.05} = 3.01$, then $\Delta\omega'$ is inside the 95% confidence ellipsoid of $\Delta\omega$, and considered to be compatible with it on the level of 95% probability. Likewise, if $Y_2 < F_{3,25,0.05} = 2\ 99$, then $\Delta\omega$ is inside the 95% confidence ellipsoid of $\Delta\omega'$, and considered to be compatible with it on the level of 95% probability. If both $\Delta\omega'$ and $\Delta\omega$ are compatible with each other on the level of 95% probability, then we are quite confident that the model is insensitive to the omission of that single datum and hence the model is robust against the datum removed. Apart from the global solution achieved from both rates and trends, we will also present the trend-only solution with omitting all rates to further demonstrate the robustness of our model from the whole data set (See below).

4 Results

The data set in table 1 was inverted to achieve a correction vector for the NNR-NUVEL1A angular velocities, and, in turn, a set of angular velocities of plates relative to hotspots by adding the correction vector to the NNR-NUVEL1A angular velocity vectors for individual plates. In the columns 9 and 10 of table 1 listed are Y_1 and Y_2 values as obtained by omitting the datum in the corresponding row. Notice that both Y_1 and Y_2 are much smaller than the critic values given above, implying that removing a single datum will not cause any significant change in the solution at a significance level 0.05; even the trend-only solution (See below) with all rates omitted is still compatible with the final solution obtained from the whole data set on the 95% probability level and inside the 95% confidence ellipsoid of final solution. So we conclude that the plate motion model we achieved is very stable and robust at all events.

4.1 Angular Velocities Obtained from the Whole Data Set

The absolute plate motion model achieved using the whole data set, designated as APM2, consists of a set of angular velocities in the hotspot frame, which are tabulated in table 2 and illustrated in figure 2.

Tab. 2　Angular Velocities for the Model APM2

Plate	Angular Velocity			Standard Deviation			Error Ellipse			Rms Velocity
	°N	°E	ω/(°)·Ma^{-1}	σ_φ/(°)	σ_λ/(°)	σ_ω/(°)·Ma^{-1}	σ_{max}/(°)	σ_{min}/(°)	ζ_{max}/(°)	(mm·a^{-1})
Africa	46.849	−44.372	0.101 5	9.41	12.70	0.013 4	14.47	6.36	122.27	9.86
Antarctica	46.871	146.942	0.084 6	9.54	13.48	0.017 7	13.67	9.27	103.01	7.11
Arabia	30.976	14.563	0.459 9	2.21	1.77	0.015 2	2.27	1.70	18.88	26.61
Australia	18.776	43.344	0.650 3	1.36	1.54	0.013 6	1.69	1.17	55.21	65.54
Caribbean	−42.303	−100.130	0.089 2	9.07	17.36	0.009 8	17.64	8.50	101.73	9.26
Cocos	20.666	−118.366	1.346 9	0.47	0.86	0.014 7	0.86	0.47	95.80	67.86
Eurasia	27.291	−171.925	0.065 5	10.29	11.30	0.020 6	12.49	8.80	53.07	6.83
India	30.623	19.024	0.468 0	2.16	1.82	0.014 9	2.26	1.68	26.74	42.39
Juan de Fuca	−35.078	64.522	0.842 3	0.69	1.59	0.015 1	1.59	0.68	89.34	22.68
Nazca	46.976	−103.824	0.547 0	1.02	3.05	0.014 4	3.05	1.01	92.67	55.94
N.America	−63.819	−80.173	0.177 6	4.02	14.36	0.012 4	14.36	4.01	88.88	15.99
Pacific	−60.063	102.210	0.833 0	0.81	2.69	0.013 3	2.72	0.69	80.66	83.53
Philippine	−47.681	−25.997	0.953 0	0.86	1.12	0.018 2	1.14	0.84	76.62	60.50
Rivera	17.319	−108.156	1.813 3	0.37	0.65	0.013 2	0.66	0.35	101.36	30.50
Scotia	−81.301	−136.758	0.226 0	4.20	27.69	0.012 2	27.78	3.54	94.71	13.94
S.America	−69.723	145.279	0.213 7	5.01	10.72	0.012 4	11.14	4.00	73.12	22.57
NNR-NUVEL1A	−49.423	90.625	0.198 3	3.06	8.89	0.013 5	8.97	2.80	81.72	

The covariance matrix of the correction vector for the NNR-NUVEL1A angular velocities in Cartesian coordinates in units of 10^{-10} rad^2 Ma^{-2} is

$$\begin{bmatrix} \sigma^2_{\omega_x} & \sigma_{\omega_x\omega_y} & \sigma_{\omega_x\omega_y} \\ \sigma_{\omega_y\omega_x} & \sigma^2_{\omega_y} & \sigma_{\omega_y\omega_z} \\ \sigma_{\omega_z\omega_x} & \sigma_{\omega_y\omega_z} & \sigma^2_{\omega_z} \end{bmatrix} = \begin{bmatrix} 1\,221.6 & -63.1 & -292.2 \\ -63.1 & 366.7 & -99.8 \\ -292.2 & -99.8 & 529.9 \end{bmatrix}$$

The model APM2 is characterized in general by slow motions. The Pacific is moving at a rate of (0.833 0°±0.013 3°)/Ma about a pole at 60.063°S, 102.210°E; Africa has a motion of (0.101 5°±0.013 4°)/Ma about a pole at 46.849°N, 44.372°W; Caribbean is moving at a rate of (0.089 2°±0.009 8°)/Ma about a pole at 42.303°S, 100.130°W; Antarctic has a motion of (0.084 6°±0.017 7°)/Ma about a pole at 46.871°N, 146.942°E; Eurasia has an even slower motion of (0.065 5°±0.020 6°)/Ma

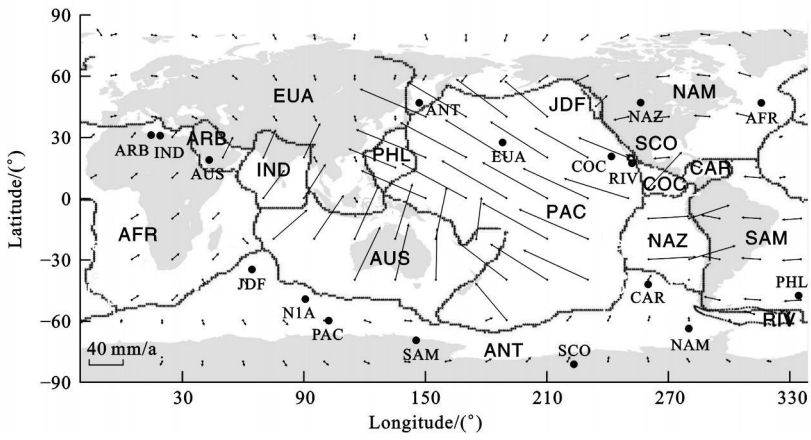

AFR— African; ANT— Antarctic; ARB— Arabian; AUS— Australian; CAR— Caribbean; COC— Cocos; EUA— Eurasian; IND— Indian; JDF— Juan de Fuca; NAM— North American; NAZ— Nazca; PAC— Pacific; PHL— Philippine; RIV— Rivera; SCO— Scotia; SAM— South American; N1A— NNR-NUVEL1A; Mercator Projection; Velocities are in mm/a; Poles of Plates(Solid Circle) in the Hotspot Frame are also Shown

Fig. 2 Plate Velocities Relative to Hotspots Computed from Model APM2

about a pole at 27.291°N, 171.925°W.

The mean rms velocity over the globe is 46.94 mm/a. The rms velocities for each plate are listed in last column of table 2 and depicted in figure 3 as a function of the percentage of the plate area that is continental and the approximate percentage of plate boundary that is attached to a subducting slab, respectively.

Our model again warrants the often-published conclusions (e.g.[2]): ①plate velocity correlates negatively with the continent area; ②plate velocity correlates positively with the fraction of the boundary being subducted; ③plate velocity correlates positively with the geographic colatitude.

The comparison of the APM2 with other models may be outlined as follows: Our Pacific motion is agreeable to the model AM1[1] of 0.84°/Ma about a pole at 67.3° S, 120.6° E; Our African motion is fairly comparable to the revised African plate motion in [31] thereby African has since 9 Ma BP a motion of 0.11°/Ma about a pole at 38°N, 61°W; Our African motion is also close to the Model A in [32] where the rotation angle during 10 Ma is 1.0° around a stage pole at 52.0°N, 16.3°W.

Our South American velocity is close to the model AM1[1] of a pole at 61.7° S, 173.9°W and a rotation rate of 0.20°/Ma, and it also may be compared with model P073[3] with a pole at 70.7° S, 131.3°W and a rotation rate of 0.232°/Ma.

In the comparison of the APM2 with the HS3-NUVEL1A[5] we have $Y_1 = 94.9 \gg F_{3,10,0.05} = 3.71$, and $Y_2 = 9.8 > F_{3,25,0.05} = 2.99$, indicating

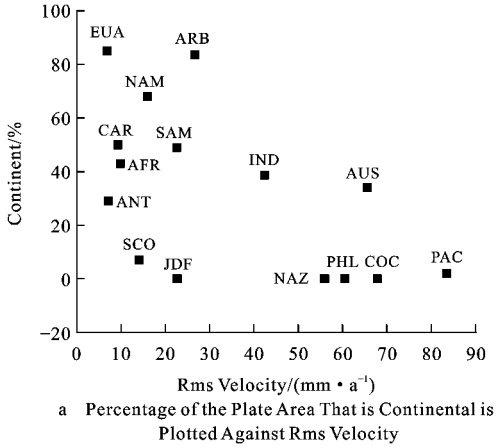

a Percentage of the Plate Area That is Continental is Plotted Against Rms Velocity

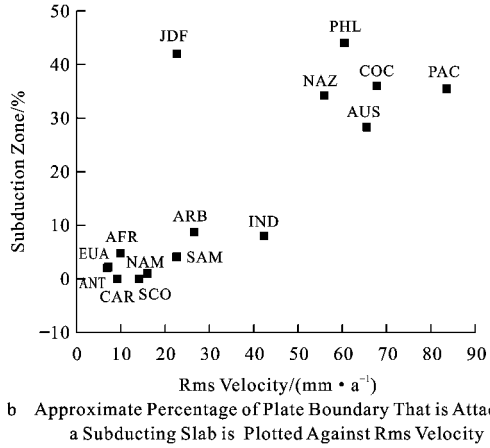

b Approximate Percentage of Plate Boundary That is Attached to a Subducting Slab is Plotted Against Rms Velocity

Fig. 3 Plate Parameter Plotted Against Rms Velocity

that the HS3-NUVEL1A velocities are far outside 95% confidence ellipsoid of APM2 velocities, and vice versa. It follows that these two models are by no means compatible on the 95% probability. Compared with the HS3-NUVEL1A, the APM2 velocities are lower by about 10% ~70% for all plates but Cocos and Nazca, for which the APM2 velocities are higher by 16% and 69% respectively. The significant difference in angular velocity between these two models is obviously ascribed to the fact that we use both the Indo-Atlantic and the Pacific hotspots rather than only use the hotspots in the Pacific hemisphere like does in [5], whereas the African hotspot data are of greater importance than the Pacific hotspot data to the global absolute plate motion inversion, as often pointed out in the literature (e.g. [1]).

4.2 Angular Velocities Obtained from the Trend-only Data

We also present in table 3 angular velocities obtained from the trend-only data with the purposes of showing by contrast the robustness of the model APM2, and consequently of explaining the validity of the trend-only solutions themselves as a useful alternative model.

For the trend-only solution, we have $Y_1 = 0.11 < F_{3,17,0.05} = 3.20$, $Y_2 = 0.07 < F_{3,25,0.05} = 2.99$, implying that they are well consistent and compatible with the model APM2 as obtained from the whole data set.

Tab. 3　Angular Velocities for Trend-only Solution

Plate	Angular Velocity			Standard Deviation			Error Ellipse			Rms Velocity
	°N	°E	ω/((°)·Ma^{-1})	σ_φ/(°)	σ_λ/(°)	σ_ω/((°)·Ma^{-1})	σ_{max}/(°)	σ_{min}/(°)	ζ_{max}/(°)	(mm·a^{-1})
Africa	46.485	−43.593	0.109 1	6.76	9.75	0.024 9	11.26	3.75	122.03	10.57
Antarctica	52.040	147.060	0.084 6	15.20	14.82	0.016 2	19.44	8.53	43.92	6.73
Arabia	31.265	13.942	0.465 7	2.81	2.24	0.013 6	3.36	1.28	143.65	27.36
Australia	19.158	42.823	0.653 1	2.25	1.39	0.008 2	2.44	1.02	154.85	65.81
Caribbean	−38.765	−95.738	0.087 9	17.76	10.36	0.007 2	17.84	10.21	6.89	8.69
Cocos	20.857	−118.106	1.349 2	0.77	0.63	0.020 6	0.87	0.49	32.94	67.65
Eurasia	32.948	−167.833	0.064 4	17.29	16.47	0.018 1	23.12	5.95	43.41	6.73
India	30.932	18.376	0.473 6	2.82	2.20	0.012 7	3.33	1.30	144.75	43.17
Juan de Fuca	−34.831	64.050	0.838 8	0.91	1.14	0.024 2	1.26	0.73	121.95	22.51
Nazca	47.178	−103.002	0.552 1	0.87	1.96	0.026 7	1.96	0.86	85.77	56.49
N. America	−61.892	−77.298	0.175 0	7.82	8.18	0.015 4	8.41	7.57	122.32	15.93
Pacific	−60.138	101.658	0.826 6	0.51	1.64	0.027 5	1.66	0.45	81.00	82.85
Philippine	−47.225	−26.069	0.953 2	1.34	1.23	0.015 9	1.70	0.65	138.32	59.91
Rivera	17.455	−107.973	1.816 3	0.60	0.43	0.020 3	0.63	0.40	21.60	16.98
Scotia	−81.305	−127.097	0.220 9	4.17	24.65	0.022 0	24.69	3.92	86.66	13.26
S. America	−70.732	145.229	0.207 1	3.16	11.19	0.025 3	11.22	3.05	85.61	21.85
NNR-NUVEL1A	−49.171	88.475	0.192 4	2.33	5.55	0.027 2	5.57	2.28	84.21	

The covariance matrix of the trend-only solutions for the correction vector for the NNR-NUVEL1A angular velocities in Cartesian coordinates in units of 10^{-10} rad^2 Ma^{-2} is

$$\begin{bmatrix} \sigma^2_{\omega_x} & \sigma_{\omega_x\omega_y} & \sigma_{\omega_x\omega_y} \\ \sigma_{\omega_y\omega_x} & \sigma^2_{\omega_y} & \sigma_{\omega_y\omega_z} \\ \sigma_{\omega_z\omega_x} & \sigma_{\omega_y\omega_z} & \sigma^2_{\omega_z} \end{bmatrix} = \begin{bmatrix} 447.5 & -88.6 & -5.5 \\ -88.6 & 711.1 & -965.8 \\ -4.5 & -965.8 & 1\,727.2 \end{bmatrix}$$

4.3 Net Rotation of the Lithosphere

The plate motion model NNR-NUVEL1A, consistent with the relative motion model NUVEL1A, is defined in the mean lithosphere frame in which there is no net rotation of the lithosphere. Our model shows (cf. Tab.2 and Fig.4), the NNR-NUVEL1A has a rotation of 0.198 3°/

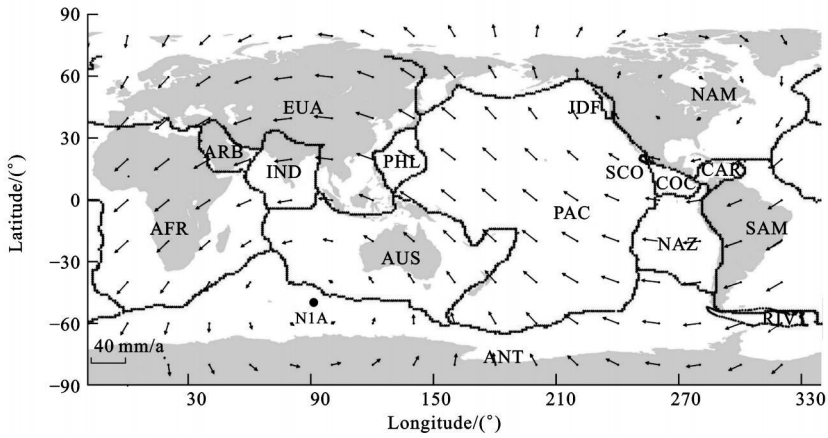

AFR— African; ANT— Antarctic; ARB— Arabian; AUS— Australian; CAR— Caribbean; COC— Cocos; EUA— Eurasian; IND— Indian; JDF— Juan de Fuca; NAM— North American; NAZ— Nazca; PAC— Pacific; PHL— Philippine; RIV— Rivera; SCO— Scotia; SAM— South American; N1A— NNR-NUVEL1A; Solid Circle Represents the Rotation Pole

Fig. 4 Net Rotation of the Lithosphere with Respect to the Deep Mantle

Ma about 49.423°S, 90.625°E, indicating the lithosphere has a net rotation this large. It follows that a significant difference exists between the mean lithosphere frame and the hotspot frame, the maximum velocity between the two reference frames being as large as 22.1 mm/a, which mostly occur in the Pacific. We are quite confident our estimation of the net lithospheric rotation is not strongly biased by improperly selecting/weighting a datum. Our net rotation of the lithosphere is comparable to the values of 0.15°/Ma about a pole at 56°S, 84°E derived by [33] using 5 observed velocities and 14 observed azimuths, and of 0.232°/Ma about 48.7°S, 80.9°E, predicted by Harper's model[34] including the net torque exerted by the subducting slabs on the lithosphere without considering any extra drag beneath continents. Our newly determined net rotation is also more close to Chase's value[3] of 0.217°/Ma about 48.2°S, 80.0°E, as cited in [34], and comparable in magnitude to the value of 0.2°/Ma about 53.8°S, 100.2°E predicted by Solomon and Sleep[35] regarding all of the drag at the base of the lithosphere concentrated beneath continental regions. Our value can be also favorably comparable to the AM1-2 rotation of 0.26°/Ma around 54°S, 66°E[2] and the Cocksworth's predicted value of 0.252°/Ma about 59°S, 48°E, as reported in [5].

5 Discussions

As shown in column 8 of table 1, the geometric contribution of a datum to the plate motion model differs numerically from one data type to another and from datum to datum. For rates the geometric contributions vary in a small range, around one Earth's radius; by contrast, for trends the differences in geometric contribution are significant, ranging from 70 to 760 Ma. Obviously, the geometric contribution values for the trends in the Pacific hemisphere are small compared to those in the Indo-Atlantic hemisphere. Hence, the trend data for the Indo-Atlantic hemisphere are expected to play a more important role in defining the global hotspot frame. To verify this, we use a small data subset consisting of only 7 Indo-Atlantic trends (St. Helena, Tristan, Vema, Reunion, Prince Edward, Discovery, Kerguelen) to invert the angular velocities of plates, with the results shown in table 4. Interestingly, the angular velocities thus obtained are well compatible with those obtained from the whole data set on the 95% probability (cf. Tabs. 2, 4) in light of $Y_1 = 0.035 < F_{3,4,0.05} = 6.59$, and $Y_2 = 0.265 < F_{3,25,0.05} = 2.99$. In other words, the angular velocities from these 7 trends are inside the 95% confidence ellipsoid of those from the whole data set. It follows

Tab. 4　Angular Velocities Obtained from 7 Trends in Indo-Atlantic Oceans

Plate	Angular Velocity			Standard Deviation			Error Ellipse			Rms Velocity
	°N	°E	ω/((°)·Ma^{-1})	σ_φ/(°)	σ_λ/(°)	σ_ω/((°)·Ma^{-1})	σ_{max}/(°)	σ_{min}/(°)	ζ_{max}/(°)	(mm·a^{-1})
Africa	47.530	−43.682	0.0975	2.20	3.20	0.0086	3.68	1.23	121.68	9.47
Antarctica	44.229	145.552	0.0854	5.56	3.61	0.0042	6.13	2.53	27.39	7.38
Arabia	30.822	15.072	0.4578	0.87	0.77	0.0050	1.08	0.43	139.70	26.16
Australia	18.579	43.681	0.6502	0.70	0.51	0.0027	0.80	0.34	148.56	65.54
Caribbean	−44.466	−102.417	0.0888	5.42	4.30	0.0028	5.91	3.59	30.27	9.44
Cocos	20.607	−118.513	1.3445	0.26	0.24	0.0062	0.31	0.15	41.34	67.97
Eurasia	24.983	−175.120	0.0660	6.41	4.82	0.0046	7.86	1.62	36.21	6.86
India	30.453	19.533	0.4662	0.87	0.76	0.0047	1.07	0.43	140.32	42.02
Juan de Fuca	−35.122	64.783	0.8451	0.30	0.42	0.0075	0.47	0.21	119.19	22.93
Nazca	47.015	−104.241	0.5438	0.28	0.74	0.0084	0.75	0.26	81.17	55.64
N.America	−65.095	−81.289	0.1781	2.45	3.12	0.0051	3.24	2.29	67.74	15.89
Pacific	−59.932	102.391	0.8366	0.16	0.54	0.0089	0.55	0.13	80.02	83.90
Philippine	−47.908	−25.828	0.9525	0.47	0.37	0.0047	0.56	0.22	144.92	60.84
Rivera	17.276	−108.251	1.8104	0.20	0.16	0.0062	0.22	0.13	34.86	17.61
Scotia	−81.494	−142.933	0.2280	1.07	9.30	0.0073	9.31	1.04	88.62	14.49
S.America	−69.069	144.254	0.2169	1.02	2.82	0.0085	2.84	0.99	84.57	22.91
NNR-NUVEL1A	−49.146	91.485	0.2020	0.67	1.87	0.0088	1.87	0.66	86.48	

that the global hotspot reference frame is almost completely defined by the Indo-Atlantic hotspots whose surface traces have very low progression rates.

As seen in table 1, the rate misfit, or the observed − modeled rate for Hawaii is as large as (22.7±5.2) mm/a, demonstrating the inconsistency of the Hawaii hotspot with the Indo-Atlantic hotspots. Knowing that the hotspot reference frame is defined essentially by the Indo-Atlantic hotspots as mentioned in previous section and that missing plate boundaries and other errors in the plate circuits only play a small role in the hotspot inconsistency[19], the misfit of (22.7±5.2) mm/a possibly quantify the relative motion of the Hawaiian hotspot relative to the Indo-Atlantic hotspots[9], also likely reflect southward motion of the Hawaiian-Emperor hotspot relative to the Pacific plate between 81 and 43 Ma[11,18]. Also, as seen from table 1, the rate misfit for Foundation is (−13.5±8.5) mm/a. The APM2 rate of the Pacific plate over the Louisville hotspot (50.5 S, 139.2 W from[36]) is (79.4±1.4) mm/a, the measured rate is (64.1±1) mm/a[27], the difference being (−15.3±1.7) mm/a. The minus residuals of observed rates for these two hotspots likely manifest themselves as southeastward motions of the hotspots in central and south Pacific Ocean, probably connected with a "demi-tour" or U-turn of mantle flow west of the East Pacific Ridge, shifting the mantle upwelling center eastward[37].

The rate misfits for the Pacific hotspots involved, ranging form (22.7±5.2) mm/a for the Hawaii in north Pacific to (−13.5±8.5) mm/a for Foundation in central Pacific, roughly correlate positively with the latitude and negatively with the longitude of the hotspots (cf. Fig. 5), implying that the relative motions of the Pacific hotspots relative to the Indo-Atlantic hotspots are spatially progressively slow down from northwest to southeast. This tends to disagree with the often-cited view that the Hawaii and Louisville hotspots have been stationary with respect to one

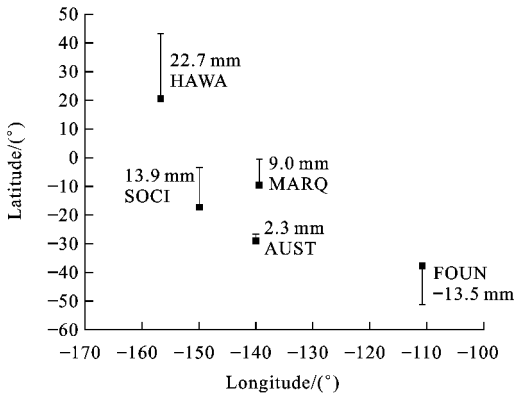

HAWA— Hawaii; SOCI— Society; MARQ— Marquesas; AUST— Austral Island; FOUN— Foundation

Fig. 5 Observed Minus Modeled Values for the Progression Rates of Volcanism in the Pacific Ocean

another since 65 Ma[19, 38] or for at least the past 21 Ma[27]. The difference in rate misfit of (38.0 ± 5.5) mm/a between Hawaii and Louisville strongly supports the view that the Pacific hotspots have an incoherent motion at least for the past 8 Ma.

6 Conclusions

The primary conclusions of this study can be summarized as follows:

(1) Two reference frames have been involved in inversion. One is the hotspot frame assuming the hotspots are fixed with respect to each other; the other is the no-net-rotation frame requiring there be no net-rotation of the lithosphere. The angular velocities of a plate can be transformed between the two frames by a linear vector equation.

(2) Knowing the hotspots move, we cannot choose but to use the fixed hotspot frame to estimate the plate motion. An attempt has been made to define a mean hotspot (or mesosphere) reference frame in terms of more globally distributed hotspots. Eventually, it was found that the mean hotspot frame is almost completely defined by the trends of the Indo-Atlantic volcanic chains which have low progression rates, and that the Pacific hotspots only play a very small role in defining the reference frame.

(3) The model APM2 has been achieved using a data set containing 8 rates and 20 trends, with the NNR-NUVEL1A as the initial model. The solution is found to be very stable and robust against the observations. The model is compatible with the trend-only, even with the 7 Indo-Atlantic trend-only solutions, on the 95% probability. The model APM2 is characterized on the whole by slow motions, favorably comparable to other models.

(4) The model APM2 again warrants the often-published conclusions: ① plate velocity correlates negatively with the continent area; ② plate velocity correlates positively with the fraction of the boundary being subducted; ③ plate velocity correlates positively with the geographic colatitude.

(5) As a useful by-product, the net-rotation of the lithosphere has been achieved with the rate being (0.198 3° ± 0.013 5°)/Ma and the pole at 49.423°S, 90.625°E, which are close to the published figures in literature.

(6) It has demonstrated that the hotspot tracks in the Pacific Ocean are inconsistent with those in the Indo-Atlantic Ocean. The misfits of the progression rates of volcanism in the Pacific Ocean exhibit roughly a positive correlation with the latitude and a negative correlation with the longitude of the hotspots, showing that the Pacific hotspots involved have incoherent motions at least during the period of the study.

References:

[1] Minster J B, Jordan T H, Molnar P, et al. Numerical Modeling of Instantaneous Plate Tectonics[J]. Geophysical Journal of the Royal Astronomical Society, 1974, 36: 541-576.

[2] Minster J B, Jordan T H. Present-day Plate Motions[J]. Journal of Geophysical Research, 1978, 83(B11): 5331-5354.

[3] Chase C G. Plate Kinematics: the Americas, East Africa, and the Rest of the World[J]. Earth and Planetary Science Letters, 1978, 37(3): 355-368.

[4] Gripp A E, Gordon R G. Current Plate Velocities Relative to the Hotspots Incorporating the NUVEL-1 Global Plate Motion Model[J]. Geophysical Research Letters, 1990, 17: 1109-1112.

[5] Gripp A E, Gordon R G. Young Tracks of Hotspots and Current Plate Velocities[J]. Geophysical Journal International, 2002, 150(2): 321-361.

[6] Wilson J. A Possible Origin of the Hawaiian Islands[J]. Ca-

nadian Journal of Physics, 1963, 41: 863.

[7] Morgan W J. Convection Plumes in the Lower Mantle[J]. Nature, 1971, 230: 42-43.

[8] Müller R D, Royer J Y, Lawver L A. Revised Plate Motions Relative to the Hotspots from Combined Atlantic and Indian Ocean Hotspot Tracks[J]. Geology, 1993, 21(3): 275-278.

[9] Molnar P, Stock J. Relative Motions of Hotspots in the Pacific, Atlantic and Indian Oceans Since Late Cretaceous Time [J]. Nature, 1987, 327: 587-591.

[10] Pollitz F F. Episodic North America and Pacific Plate Motions[J]. Tectonics, 1988, 7(4): 711-726.

[11] Tarduno J A, Cottrell R D. Paleomagnetic Evidence for Motion of the Hawaiian Hotspot During Formation of the Emperor Seamounts[J]. Earth and Planetary Science Letters, 1997, 153(3): 171-180.

[12] Wessel P, Kroenke L W. Ontong Java Plateau and Late Neogene Changes in Pacific Plate Motion[J]. Journal of Geophysical Research, 2000, 105(B12): 28255-28277.

[13] Gordon R G, Jurdy D M. Genozoic Global Plate Motions[J]. Journal of Geophysical Research, 1986, 91(B12): 12389-12406.

[14] Morgan W J. Hotspot Tracks and the Early Rifting of the Atlantic[J]. Tectonophysics, 1983, 94: 123-139.

[15] Duncan R A. Hotspots in the Southern Oceans——an Absolute Frame of Reference for Motion of the Gondwana Continents[J]. Tectonophysics, 1981, 74(1/2): 29-42.

[16] Mcdougall I, Duncan R A. Age Progressive Volcanism in the Tasmantid seamounts[J]. Earth and Planetary Science Letters, 1988, 89(2): 207-220.

[17] Duncan R A, Richards M A. Hotspots, Mantle Plumes, Flood Basalts, and True Polar Wander[J]. Reviews of Geophysics, 1991, 29(1): 31-50.

[18] Tarduno J A, Duncan R A, Scholl D W, et al. The Emperor Seamounts: Southward Motion of the Hawaiian Hotspot Plume in Earth's Mantle[J]. Science, 2003, 301: 1064-1069.

[19] Divenere V, Kent D V. Are the Pacific and Indo-Atlantic Hotspots Fixed? Testing the Plate Circuit Through Antarctica[J]. Earth and Planetary Science Letters, 1999, 170(1/2): 105-117.

[20] Argus D F, Gordon R G. No-net-rotation Model of Current Plate Velocities Incorporating Plate Motion Model NUVEL-1 [J]. Geophysical Research Letters, 1991, 18: 2039-2042.

[21] Demets C, Gordon R G, Argus D F, et al. Effect of Recent Revisions to the Geomagnetic Reversal Time Scale on Estimates of Current Plate Motions[J]. Geophysical Research Letters, 1994, 21: 2191-2194.

[22] Brozena J M. Temporal and Spatial Variability of Seafloor Spreading Processes in the Northern South Atlantic[J]. Journal of Geophysical Research, 1986, 91(B1): 497-510.

[23] Pollitz F F. Two-stage Model of African Absolute Motion During the Last 30 Million Years[J]. Tectonophysics, 1991, 194(1/2): 91-106.

[24] Mcdougall I, Duncan R A. Linear Volcanic Chains —— Recording Plate Motions? [J]. Tectonophysics, 1980, 63(1/4): 275-295.

[25] Pollitz F F. Pliocene Change in Pacific-plate Motion[J]. Nature, 1986, 320: 738-741.

[26] Antretter M, Steinberger B, Heider F, et al. Paleolatitudes of the Kerguelen Hotspot: New Paleomagnetic Results and Dynamic Modeling[J]. Earth and Planetary Science Letters, 2002, 203(2): 635-650.

[27] O'Connor J M, Stoffers P, Wijbrans J R. Migration Rate of Volcanism Along the Foundation Chains, SE Pacific[J]. Earth and Planetary Science Letters, 1998, 164(1): 41-59.

[28] O'Connor J M, Stoffers P, Bogaard P, et al. First Seamount Age Evidence for Significantly Slower African Plate Motion Since 19 to 30 Ma[J]. Earth and Planetary Science Letters, 1999, 171(4): 575-589.

[29] DeMets C, Gordon R G, Argus D F, et al. Current Plate Motions [J]. Geophysical Journal International, 1990, 101: 425-478.

[30] Steinberger B. Plumes in a Convecting Mantle: Models and Observations for Individual Hotspots[J]. Journal of Geophysical Research, 2000, 105(B5): 11127-11152.

[31] O'Connor J M, Roex A P. South Atlantic Hot Spot-plume System: 1. Distribution of Volcanism in Time and Space[J]. Earth and Planetary Science Letters, 1992, 113(3): 343-364.

[32] O'Connor J M, Duncan R A. Evolution of the Walvis Ridge-Rio Grande Rise Hot Spot System: Implications for African and South American Plate Motions over Plumes[J]. Journal of Geophysical Research, 1990, 95(B11): 17475-17502.

[33] Ricard Y, Doglioni C, Sabadini R. Differential Rotation Between Lithosphere and Mantle: a Consequence of Lateral Mantle Viscosity Variations[J]. Journal of Geophysical Research, 1991, 96(B5): 8407-8415.

[34] Harper J F. Mantle Flow and Plate Motions[J]. Geophysical Journal of the Royal Astronomical Society, 1986, 87: 155-171.

[35] Solomon S C, Sleep N H. Some Simple Physical Models for Absolute Plate Motions[J]. Journal of Geophysical Research, 1974, 79(17): 2557-2567.

[36] Lonsdale P. Geography and History of the Louisville Hotspot Chain in the Southwest Pacific[J]. Journal of Geophysical Research, 1988, 93(B4): 3078-3104.

[37] Gaboret C, Forte A M, Montagner J P. The Unique Dynamics of the Pacific Hemisphere Mantle and Its Signature on Seismic Anisotropy[J]. Earth and Planetary Science Letters, 2003, 208(3/4): 219-233.

[38] Watts A B, Weissel J K, Duncan R A, et al. Origin of the Louisville Ridge and Its Relationship to the Eltanin Fracture Zone System[J]. Journal of Geophysical Research, 1988, 93(B4): 3051-3077.